MDPI

Article

Cylindrical Cavity Sensor for Distinction of Various Driveability Index Gasoline With Temperature Robustness

Chong Hyun Lee [1,*], Yoon-Sang Jeong [1] and Hina Ashraf [1,2]

[1] Department of Ocean System Engineering, Jeju National University, Jeju 690-756, Korea; chonglee@jejunu.ac.kr (C.H.L.); jyssolt@naver.com (Y.J.)

[2] Department of Electrical Engineering, National University of Computer and Emerging Sciences, Foundation for Advancement of Science and Technology (NUCES-FAST), H 11/4, Islamabad 44000, Pakistan ; hina.ashraf@nu.edu.pk (H.A.)

* Correspondence: chonglee@jejunu.ac.kr; Tel.: +82-10-3359-3085

† Current address: Jeju National University, 102 Jejudaehak-ro, Jeju-si, Jeju Special Self-Governing Province, 63243, Korea

Version October 14, 2019 submitted to Sensors

Abstract: In this paper, a cylindrical cavity sensor based on microwave resonant theory is proposed to distinguish between various driveability index gasolines under temperature variations. The working principle of the proposed sensor is based on the fact that change in permittivity of gasoline samples inside cavity sensor can also cause a change in resonant frequency. The proposed sensor has good sensitivity in terms of resonant frequency separation which enables it to capture the minute permittivity changes and distinguish different gasolines. By using normal gasoline permittivity of 2.15 and changing sensor parameters, the sensor is designed by high-frequency structure simulator (HFSS). The designed sensor has resonant frequency of ~~the sensor is~~ 7.119 GHz for TM_{012} mode with 19.2mm radius, 35mm height and one port coupling probe of 8mm height. The proposed cylindrical cavity sensor shows advantages of excellent resonant characteristics of small cavity size and small sample amount. To optimize and verify parameters of the sensor, many experiments have been carried out by using HFSS and vector network analyzer (VNA). Consequently, the proposed sensor is proven to be robust to temperature changes in terms of resonant frequency separation. The minimum frequency separation to distinguish gasoline samples is found to be larger than 29 MHz with reflection coefficients under -11 dB for temperature changes from -35C to 0C. The consistency of experimental and theoretical results also are presented, which guarantees accuracy of the sensor for distinction gasoline.

Keywords: driveability index (DI); normal gasoline; permittivity; sensitive microwave sensor

1. Introduction

Gasoline is a complex combination of chemical components used as fuel for spark-ignition engines [1]. The performance of gasoline over the entire range of operating temperatures is measured by the driveability index (DI) [2], [3]. A parametric study on fuel has shown that DI is closely related to fuel volatility and has a significant impact on engine cold start performance [4]. DI is a measure of fuel volatility that is a function of ethanol content and temperature ranges at which 10% (T10), 50% (T50) and 90% (T90) of the gasoline boils. The DI of fuel purchased is correlated with ambient temperature. The vehicles that use different blends of gasoline require some form of sensors to measure the DI and composition of fuel. For such ~~kind of~~ measurements, highly accurate and sensitive sensors are required, however the traditional sensors performance is insufficient to meet these criteria. At present, different techniques have been used to measure DI of the fuel. Lambert et. al. estimates the DI of the sample by heating fuel sample placed between two

narrow parallel plates of a capacitor and then measuring the change in capacitance of the sensing element as a function of time and temperature [5]. Another reported technique utilized platinum resistance temperature detectors (RTDs) to compare the engine exhaust gas temperatures during cold starts to actual engine exhaust air/fuel ratios using low and high DI fuels to detect the cold start volatility characteristic of the fuel [6]. The limitation to this technique is that it can only detect the presence of HiDI fuel and can not differentiate between various HiDI. Moreover, both of the techniques mentioned above generally require the sample to be heated for a substantial amount of time before the sensor becomes effective for control following a cold start. ~~On the contrary~~, RF techniques does not require the sample to be heated so the quick measurements are possible.

The gasoline driveability index (DI) sensor is used ~~at the start of~~ a vehicle. It should be small in size for mounting in vehicle and for fast measurements. ~~In this regard,~~ conventional analysis technology based on gas chromatography/mass spectrometry can analyze sample with high resolution, ~~However,~~ this ~~analysis~~ process is complicated and time consuming [7], [8]. In comparison, radio frequency and microwave technologies are fast and simple processes. Therefore, ~~radio frequency and microwave technologies~~ are efficient and cost effective approaches for DI sensing. Recently, many researches are proposed ~~that incorporates~~ microwave based techniques to identify and observe different liquid samples [9], [10], [11]. The sensing occurs when the solution undergoes interaction with propagating or resonating modes of electromagnetic waves. Due to this interaction, the complex permittivity of the material changes and it manifests itself as a frequency change, attenuation, reflection of the signal or a phase shift. The sensing principle relies on the changes of the device response in terms of the transmitted power, resonant frequency and 3-dB bandwidth. Among these techniques, spectroscopy is a commonly used technique to measure permittivity of liquid samples as a function of frequency that gives information about relative permittivity and loss tangent of sample [12]. It is being used to distinguish between materials but the sensitivity is not high and can sense the variation of permittivity values from 3 to 11 for resonant frequency change of 5.2 GHz to 4.1 GHz [13]. Since the gasoline sensor needs to be small, microwave technologies help to make sensor compact and more configurable than mass spectrometry and gas chromatography.

Among microwave based designs, resonant cavities are easy to fabricate, requires minimal sample, possess excellent resonant characteristics that ensure higher accuracy [14], [15], high sensitivity [16] when used explicitly in sensing resonant frequency locations corresponding to the cavity of half a wavelength long and can be used for different material characterisation such as: for nutrient monitoring in waste water treatment [17], food evaluation and analysis [18]. It is worth noting that the resonant frequency is comparatively less sensitive to the impurities that increase the conductivity of fuel blends [19]. Many researches are based on cavity designs. Guo et. al. in [14] used cylindrical cavity opened at both ends for on-line water content measurement by measuring resonant frequency of the cylindrical cavity. Another reported sensor utilizes a cylindrical cavity for resonant frequency change between 5 and 5.7 GHz to analyze a two phase gas–liquid flow regime in a pipeline [20]. Ethanol content present in gasoline has high permittivity that allows useful sensors to be built using relatively short lengths of metal enclosure cavities [19].

In this paper, a microwave based sensor is proposed with high sensitivity and accuracy for the distinction of various gasoline. The difference of permittivity values between different gasoline is extremely minor ranging from 0.05 to 0.15, which requires high sensitivity. The sensor is optimized to have a specific resonant frequency according to unique permittivity of the each gasoline sample and the unknown sample can be found by comparing this resonant frequency with known samples. For the sensor design, a one port cylindrical cavity sensor is adopted, which results in small size and low cost. ANSYS high-frequency structure simulator (HFSS) and vector network analyzer (VNA) are used to verify the design and performance of proposed cylindrical cavity sensor. The novel contribution of the presented sensor is its robustness with temperature variations while maintaining sensitivity and accuracy.

The content of the paper is organized as follows. Section 2 presents proposed sensor modeling and cylindrical cavity theory. Section 3 presents the design procedure, structural parameters and simulation analysis performed by HFSS. In Section 4, experimental setup is described and the performance evaluation of

the proposed sensor on the basis of simulation and experimental results is discussed. The conclusion of the paper is presented in Section 5.

2. Sensor Modeling and Design

To distinguish between various gasoline, the proposed sensor model is shown in Figure 1. This sensor can be separated into two components: a monopole and a cylindrical cavity which can be built from circular waveguide by shorting metal walls at both ends. Figure 1a illustrates the geometrical structure of the cylindrical cavity resonator which consists of closed copper cylinder filled with sample of permittivity ϵ, where $\epsilon = \epsilon_0\epsilon_r$ (ϵ_0 is permittivity of free space approximately equals to 8.85×10^{-12} F/m and ϵ_r is the relative permittivity of fuel). The proposed sensor design is chosen to be closed metal cavity structure to avoid any external interaction since the sensor is to be used in either inside fuel tank or at the fuel inlet of car where there is a chance of presence of other electromagnetic waves. The interior of the cavity is a hollow uniform cylindrical shape. A small hole is kept at the top center of cylindrical cavity for providing the feed source. The feed source is vertically placed into the cavity through the hole which acts as an intermediator from outside equipment to cavity for transmitting microwaves inside the metal enclosure and for monitoring its resonant behaviour. A monopole has been chosen as a feed source as shown in Figure 1b. The degree of coupling is controlled by adjusting the length of the probe which is kept smaller to have minimum interaction with the field inside. The monopole is coated with thin layer of insulating medium Teflon to avoid direct contact with the testing gasoline samples in order to avoid corrosion which may lead sensor to operate abnormally. Even though the current in monopole is very small, an electric field is created between monopole and adjacent wall of the resonator which is maximum at the location of monopole and also perpendicular to the wall. The current also generates a magnetic field that radiates like a magnetic dipole tangential to the wall.

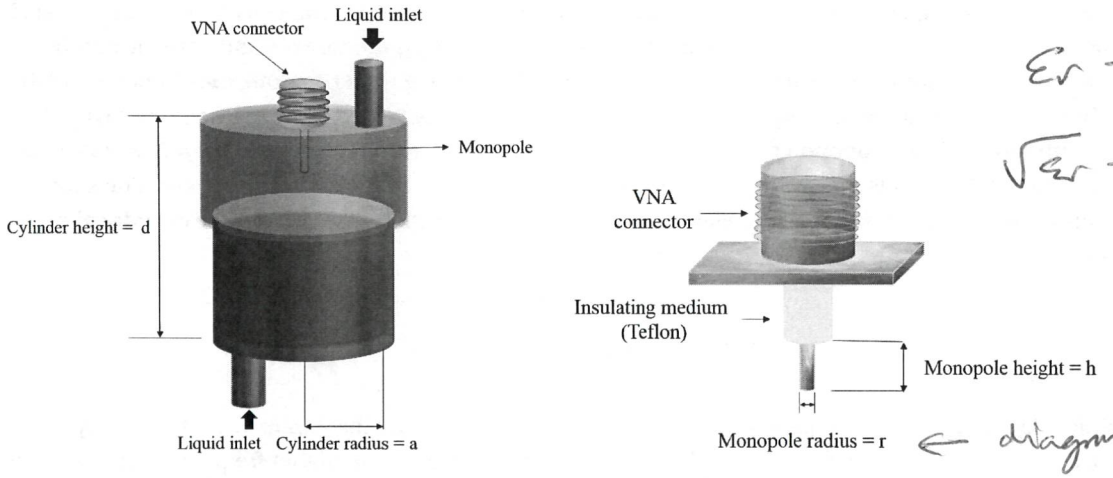

Figure 1. Geometrical structure of **(a)** Cylindrical cavity resonator **(b)** A coupling probe (monopole) fixed at the top center of cavity

The resonant frequency of the cavity exhibits a substantial change with a small change in permittivity of gasoline samples. A basic experimental schematic utilizing the proposed sensor for measuring permittivity of different gasoline samples is shown in Figure 2.

2.1. Cylindrical Cavity Sensor Theory

When resonance occurs, there is possibility of occurrence of various electromagnetic modes within a specific cavity where different modes have their own resonant frequencies, dimensions of cavities and associated Q-values [21]. The basic modes for cylindrical cavity resonators are transverse magnetic TM_{01} and transverse electric TE_{01} and TE_{11} [22]. In microwave theory, the higher-order mode decays rapidly, hence

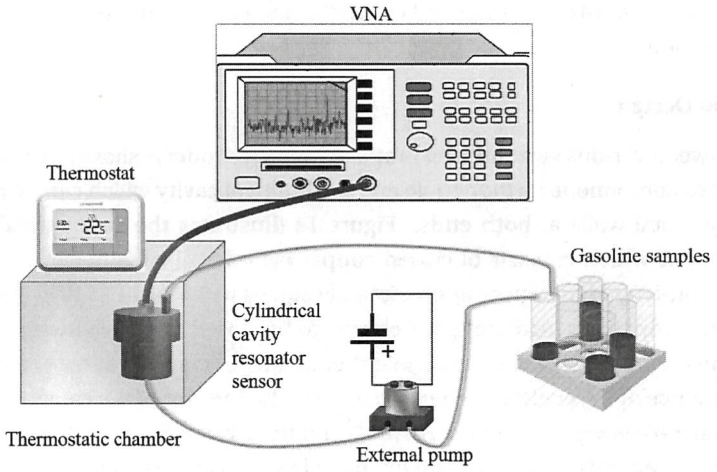

Figure 2. Experimental schematics of microwave cavity resonator for measuring permittivity of different gasoline samples

TM_{01}, the first higher mode of the circular waveguide, was selected. This selection was made since it is easier to manufacture as compared to the TE mode in actual application environment. In cylindrical cavity, the wavelength of the TM_{01} mode can be defined as [23]:

$$\lambda = 2.612a \tag{1}$$

where a is the radius of the cavity ~~from inside~~. The resonant frequency for a given mode is calculated using Equation (2), where f_{nmt} is the resonant frequency of the TM_{nmt} mode; m, n and t are the number of full-wave patterns along the circumference, the number of half-wave patterns along the diameter and the number of half-wave along the height of the cylindrical cavity respectively; d is the height of the cavity; P_{nm} is the mth root of Bessel function of nth order. The values of P_{nm} are listed in Table 1; $c = 299792458 m/s$ is the speed of light; μ_r is the relative permeability (value considered to be 1 since the gasoline samples are non-magnetic in nature) and ϵ_r is relative permittivity of the filled material inside the cylindrical cavity sensor.

$$f_{nmt} = \frac{c}{2\pi\sqrt{\mu_r\epsilon_r}}\sqrt{(\frac{P_{nm}}{a})^2 + (\frac{t\pi}{d})^2} \tag{2}$$

Traditionally, cavity resonators are large in size and expensive to fabricate that limits their use in many major applications [14]. From Equation 2, it can be noticed that the utilization of higher frequencies may lead to small size cavities that in turn need ~~very less~~ quantity of sample. The proposed sensor design requires small amount of liquid sample to be contained within the cavity since the volume of cavity is smaller.

Table 1. The roots (P_{nm}) of the Bessel function

n \ m	1	2	3
0	2.405	5.520	8.654
1	3.832	7.016	10.174
2	5.135	8.417	11.620

3. Simulations Results of the Proposed Sensor

For transmitting and receiving electromagnetic waves, more than one antennas can be positioned inside the cavity. The most common arrangement is one-port or two-port cavities [30]. For one-port arrangement,

when the testing material inside the cavity interacts with electromagnetic waves, a part of power is reflected back which is termed as reflection coefficient or return loss that can be measured with the help of VNA. This measure is used in the following simulations and experiments to analyze the performance of proposed sensor. For sensitivity analysis, resonant frequency separation is chosen as a measure of sensitivity for distinction of gasoline samples.

3.1. Structural Parameters of the Proposed Sensor

The proposed sensor is designed to attain wide frequency separations and low reflection coefficients for all scenarios. The design steps of proposed cavity sensor are as follows:

1. Selection of permittivity (ϵ): First, we selected the permittivity of gasoline for simulating the sensor model. The gasoline samples used in our experiments are high driveablity index (HiDI) samples with average permittivity value of 2.1 and the permittivity of normal gasoline used in the design of this sensor is 2.15, which is similar to the average permittivity of HiDI gasoline.
2. Selection of cylindrical cavity mode and design frequency: The procedure of selecting TM_{012} and design frequency is already described in Section 2.1
3. Selection of monopole height (h): We have chosen the height of the monopole cavity through simulations by sweeping the radius of the cylindrical resonator for the frequency range of 6.7-7.7 GHz. Figure 3a shows the optimization process of selecting monopole height. The height of monopole is chosen to be 8mm as it gives the minimum reflection coefficient for the given frequency range.
4. Selection of cylindrical height (d): To find the best height for the design, we have observed that the height of 35 mm of cavity gives good response in terms of lower reflection coefficient as shown in Figure 3b.

Similarly, all those optimized parameters were chosen that gave best results in frequency separations and reflection coefficients.

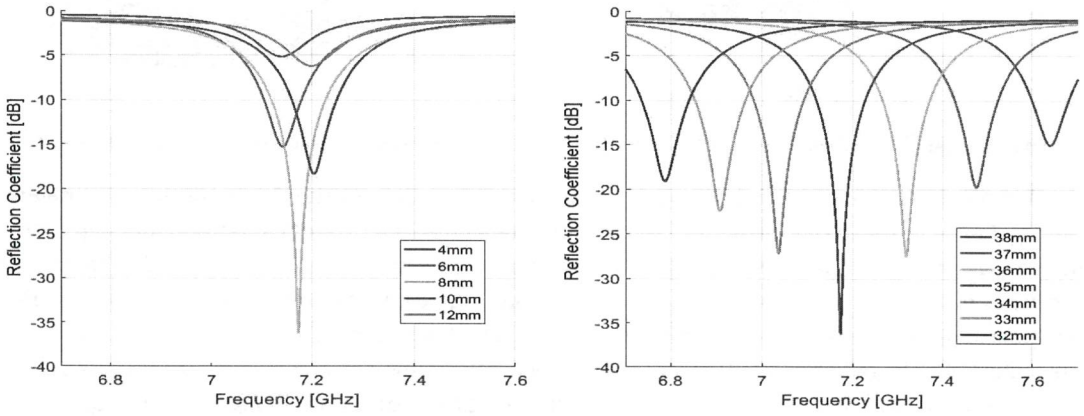

(a) **(b)**

Figure 3. (a) Simulation results for the optimization of monopole height (h) **(b)** Simulation results for the optimization of cylindrical cavity height (d)

The proposed cylindrical cavity sensor is fabricated using conductive copper cylinder of inner radius (a) 19.2 mm and height (d) 35 mm. The manufactured sensor is shown in Figure 7a. In this model, a coupling probe of height h and radius r is designed by extending the feeding coaxial cable with a small distance into the cylindrical cavity sensor and fixing at the bottom center. In our case, the height h of the probe is set to 8mm which is equal to one fourth of wavelength of frequency 7.119 GHz making the input impedance nearly equivalent to that of an open circuit. The dimensions of coupling probe are 0.5mm x 8mm and it is wrapped with Teflon with radius size of 3mm as shown in Figure 7b. The selected design parameters for the cavity resonator with height of 35mm, circumference of 120.86mm and feeding height of 8mm showed minimum

reflection coefficient and largest frequency separation. The optimized parameters for the designed sensor are given in Table 2.

Table 2. Design parameters of the proposed sensor

Parameter	Dimension (mm)	Parameter	Value
a	19.2	P_{01}	2.405
d	35	t	2
h	8	Permittivity (ϵ)	2.15
r	0.5	mode	TM

The electromagnetic field of cylindrical cavity sensor with TM_{012} mode is simulated using HFSS software in Figure 4a and 4b. It can be observed from these figures that the magnetic field of TM mode is parallel to the cavity bottom and tangent to the wall of the cylinder and the electric field is perpendicular to both the magnetic field and the wall at the location of the probe. The intensity of electric and magnetic field is maximum at the center of the cavity and decreases approaching from the cavity center to the boundary. Therefore, these simulation results are in good agreement with theory mentioned in Section 2.

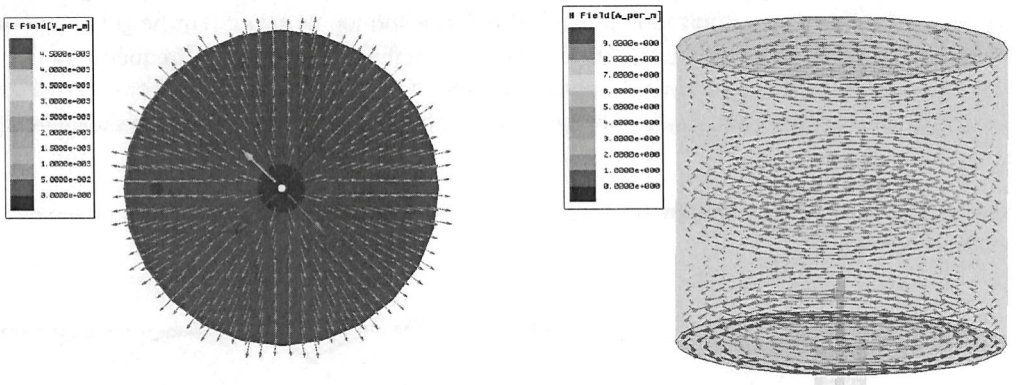

(a) **(b)**

Figure 4. (a) Electric field top view of cylindrical resonator **(b)** Magnetic field side view of cylindrical resonator

By using HFSS, simulations have been conducted to analyze how the chosen design parameters and selected TM_{012} mode for the presented sensor affect reflection coefficients and frequency separation for different gasoline. We considered five different gasoline samples among samples specified in Table 3, which represents different types of standard gasoline/ethanol blends according to their ethanol content and emissions of nitrogen oxides (NOx), total hydrocarbon (THC), non-methane hydrocarbon (NMHC), carbon monoxide (CO). The reflection coefficients of the selected five samples of LEV3, Tier3, Euro4, Cold CO, Tier2 and one assumed sample (permittivity differ by 0.01 with LEV3) are shown in Figure 5 for frequency range from 6.6 GHz to 7.7 GHz. The resonant frequency separation of four samples is greater than 100MHz and the reflection coefficients are below -12 dB. The minimum frequency separation of 18 MHz lies between the assumed sample and LEV3, which is still possible to distinguish.

Next, we simulated three different fuels such as kerosene, gasoline and heavy oil as mentioned in Table 4 with the proposed sensor to monitor the results. The reflection coefficient according to frequency is shown in Figure 6. The response is plotted for frequency range of 6 GHz to 8.5 GHz. Note that the proposed sensor exhibits remarkable resonant frequency separation between different fuel samples and has low reflection coefficients below -31 dB. Also, it can be easily observed that resonant frequency has a negative relationship with permittivity and the resonant frequency.

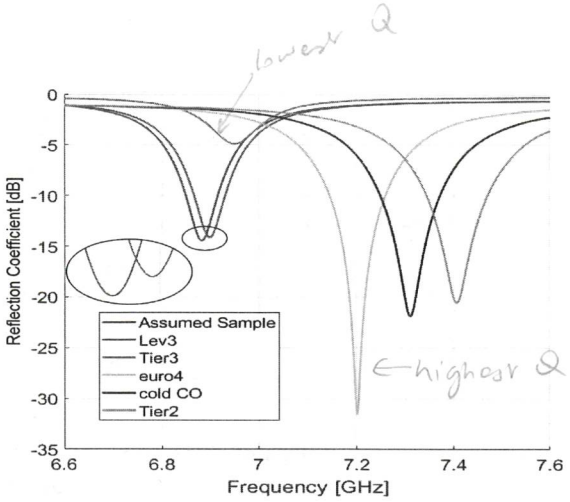

Figure 5. Simulation results of resonant frequency for the proposed sensor at 20°C temperature for various gasoline samples

Table 3. Gasoline Samples according to emission standards for light vehicles, g/km [24],[25]

Index	Gasoline Samples	CO	THC	NMHC	NOx	Ethanol (vol.%)
1	Tier 2 (Indolene)	3.5	-	2.16	4.44	< 10
2	Tier 3 (Indolene E10)	3.5	-	-	4.9	14.8-15.2
3	LEV 2 (Phase 2)	6.4	0.032	-	0.05	< 10
4	LEV 3 (Phase2 E10)	-	-	-	0.07	9.75-10.25
5	Cold CO	1.7	0.45	-	0.17	<10
6	Cold CO E10	1.5	0.4	-	0.2	10
7	Euro 4	1	0.10	-	0.08	< 10
8	Euro 5	1	0.10	0.068	0.06	< 10

4. Experimental Results and Discussions

4.1. Experimental Setup

Experimental setup consisted of cylindrical cavity resonator with monopole, VNA, external pump, thermostatic bathing, cable, capillary tubes and gasoline samples. The cylindrical cavity sensor is connected through a connector to supply microwave signals and to allow measurements to be taken using a calibrated series network analyzer VNA (100k Hz - 8.5 GHz E5063A, KEYSIGHT) via 50 Ω coaxial cable. The gasoline solutions are introduced in the cavity via a thermoplastic capillary. In particular, the capillary is connected to an external pump via tube fittings so that a continuous gasoline flow is created and no air bubbles are formed in the capillary. Thermostatic bath and thermometer are used to control and monitor the temperature of gasoline samples as shown in Figure 8b. The experimental setup described above is shown in Figure 8a showing gasoline bottles with different permittivities and microwave cavity sensor.

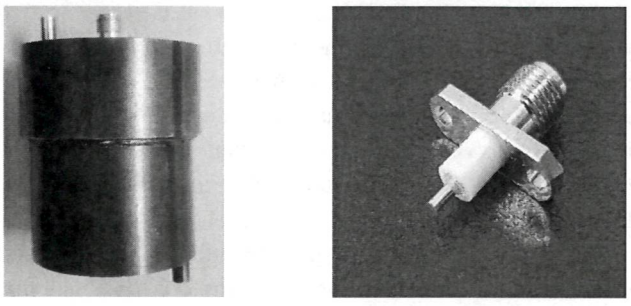

(a) **(b)**

Figure 7. (a) Actual fabricated sensor **(b)** Coupling Probe (Monopole)

	Kerosene	Gasoline	Heavy Oil
f_r (GHz)	7.847	7.173	6.519
Γ (dB)	-31.5	-36.2	-32.0
ϵ	1.8	2.15	2.6

Table 4. Simulation results of proposed sensor showing resonant frequency, reflection coefficient and permittivity for kerosene, gasoline and heavy oils [26] at room temperature (20°C).

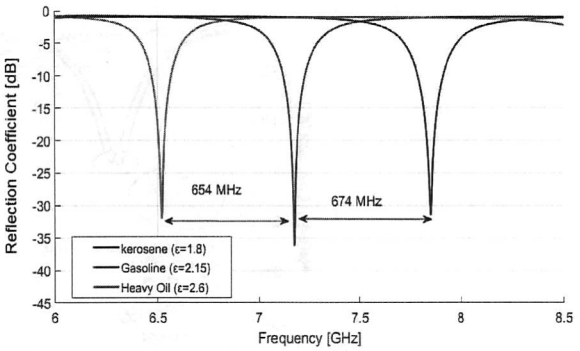

Figure 6. Reflection coefficient versus resonant frequency of the proposed sensor for kerosene, gasoline and heavy oils at room temperature (20°C).

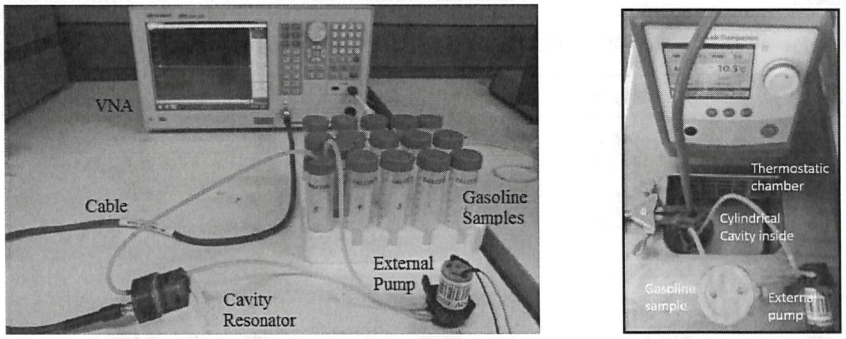

(a) **(b)**

Figure 8. **(a)** Original experimental setup **(b)** Thermostatic bathing

4.2. Results and Discussion

Two important properties of dielectric materials are complex permittivity $\epsilon^* = \epsilon - j\epsilon''$ and loss tangent $tan\delta = \frac{\epsilon''}{\epsilon}$. The real part ϵ of ϵ^* is the permittivity (i.e. product of the free space permittivity ϵ_0 and the relative real/absolute permittivity ϵ_r) quantifying the stored energy within the medium and the imaginary part ϵ'' represents dielectric loss factor related to the dissipation of energy within the medium. The ratio $tan\delta$ quantifies the loss of power due to the propagation in a conductor. To analyze this loss of power, we performed experiments with the proposed sensor on gasoline samples with different permittivities as shown in Figure 9 using Table 5. The complex permittivity values were measured using N1501A permittivity measuring kit.

As we know that the permittivity of a solution changes with change in temperature, which in turn changes the resonant frequency. However, the effects are relatively small for hydrocarbon lubrication oils. The typical decrease in permittivity for hydrocarbon oils is about 0.0013 to 0.05 percent per degree Celsius [27]. To verify this relationship and to analyze the ability of proposed sensor to distinguish various gasoline samples under different temperature conditions, we evaluated the response of the sensor as shown in Figure 10 by inducing temperature variations with the help of thermostatic bath. There is small change in resonance frequencies for the temperature variation of 0°C to -35°C for a given gasoline sample. The resonant frequency shifts towards a slightly high value with the rise in temperature for Euro4, Cold CO and Tier2. For Tier3 and LEV3, the resonant frequency shifts slightly to a lower value since these two gasoline samples have high percentage of ethanol and the ethanol tends to have low permittivity at high temperatures [28]. Nonetheless, the performance of the proposed sensor is almost same which confirms the robustness of the sensor with temperature changes. The minimum frequency separation of 31 MHz lies between Euro4 and Cold CO at 0°C temperature. The designed temperature range for the fuel tanks are between 40°C and 85°C [29]. Moreover, HiDI gasoline samples are generally

Gasoline Sample	Permittivity Real (ϵ)	Permittivity Complex (ϵ'')
Tier2	2.018	0.0764
Cold CO	2.072	0.073
Euro4	2.134	0.066
Normal gasoline	2.15	0.0494
Tier3	2.289	0.0087
LEV3	2.324	0.0385

Table 5. Real permittivity and measured complex permittivity for different gasoline samples at 20°C

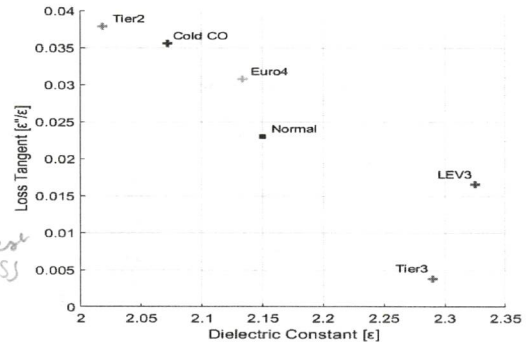

Figure 9. Variation of Loss-tangent ($tan\delta$) with permittivity (ϵ) for different gasoline samples

used in the cold areas. Therefore, the measurements are carried out for the temperature ranges of 0°C to -35°C.

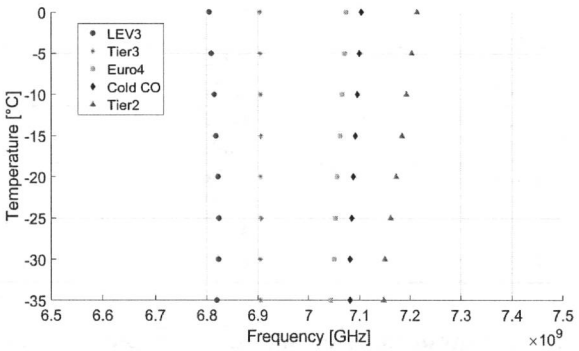

Figure 10. Experimental results of resonant frequency for the proposed sensor at different temperature for various gasoline samples

Using optimized parameters, we performed full wave analysis of the proposed sensor using HFSS for the frequency range of 6.5 GHz to 7.5 GHz under different temperature conditions. By sweeping frequency from 6.5 GHz to 7.5 GHz, we achieved reflection coefficient for LEV 3, Tier 3, Euro 4, Cold CO and Tier 2 at -35°C to 0°C temperatures as shown in Figure 11a and 11b respectively. The proposed sensor fulfills the requirement of large frequency separations between different samples making it sensitive towards small changes in permittivity of a given sample. The gasoline sample, Tier2 shows minimum reflection coefficient at -35°C with -63.64 dB dip at resonant frequency of 7.15 GHz. In Table 6, frequency separations of close resonance peaks are listed. At higher temperature, the resonant frequency is shifted to a higher value. Higher temperature increases the activity of electron particles and reduces the relative permittivity of fuels thus, resonant frequency as well as reflection coefficient increases. Here, point to be noted is that the fuel with lower permittivity has higher resonant frequency and vice versa i.e. Tier 2 as the fuel with lower permittivity and LEV 3 as the fuel with higher permittivity. These results reveal that the proposed cylindrical cavity sensor is still very sensitive to distinguish normal and HiDI gasoline under different temperature conditions.

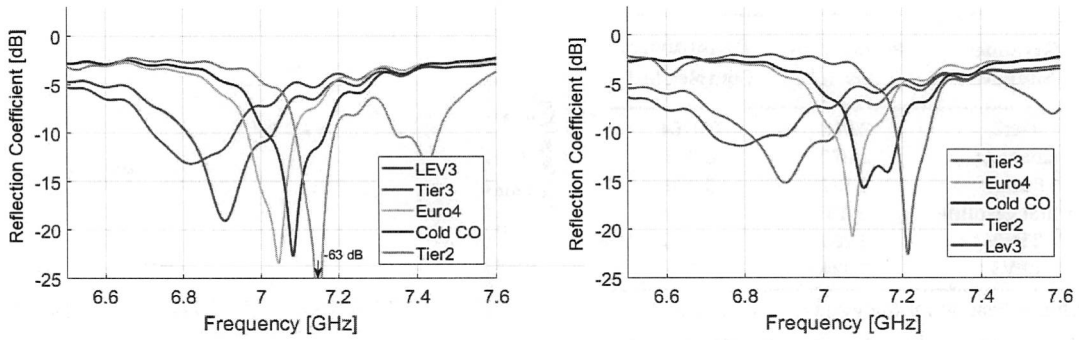

(a) **(b)**

Figure 11. Reflection coefficient analysis of the proposed sensor at temperature **(a)** -35°C **(b)** 0°C

Table 6. Frequency separation of various gasoline samples at different temperatures

Gasoline Samples	Resonant frequency [GHz]	Reflection Coefficient [dB]	Frequency Separation [MHz]
LEV 3 (-35 °C)	6.818	-13.14	86
Tier 3 (-35 °C)	6.904	-19.02	
Euro 4 (-35°C)	7.042	-23.4	36
Cold CO (-35 °C)	7.078	-22.69	
LEV 3 (0 °C)	6.791	-11.41	112
Tier 3 (0 °C)	6.903	-15.21	
Euro 4 (0 °C)	7.074	-13.36	29
Cold CO (0 °C)	7.103	-15.71	
Tier2 (-35 °C)	7.148	-63.64	-
Tier 2 (0 °C)	7.215	-22.37	

The relationship between permittivity of the different gasoline samples and resonant frequency is shown in Figure 12a where curve 1 shows theoretical values and curve 2 shows experimental values. The resonant frequencies of theoretical data are slightly higher than experimental values. The qualitative analysis of Figure 12a suggests that resonant frequency decreases monotonically with increase in permittivity in both curves. The experimental results are in agreement with that of theoretical results. Now, to perform quantitative analysis of the given data we define percentage error as follows: Percentage Error = |Experimental values - Theoretical|/Experimental values X 100

Figure 12b represents the percentage error between the theoretical and experimental values of resonance frequencies for various gasoline samples with different permittivity. The overall error is below 1.7%, which confirms the accuracy of the proposed sensor.

All the measurements were repeated five times with the same sample and their average value is considered. The measurement error of all experiments including 0°C of LEV3, which has the lowest quality factor, has an error of less than 0.5 MHz. Samples with different dielectric constants in experimental measurements show various quality factors. However, since the measurement error of all samples is 0.5 MHz, which is smaller than the minimum resonant frequency difference 29 MHz between samples, it is possible to distinguish between samples even considering the error due to the quality factor.

At the end, we have performed a comparison of our proposed method with the capacitor method, which is one of the DI measurement method presented in [5]. The results are summarized in Table 7. The sensitivities of the proposed sensor are achieved by taking the ratio of difference in resonant frequencies (fr) of the samples to the difference in DI values and listed in Table 7 a. Similarly, sensitivities of the sensor in [5] calculated by taking the ratio of voltage difference of the samples to the difference in DI values and listed in Table 7 b. It can be seen that the proposed sensor is better in terms of sensitivity to DI.

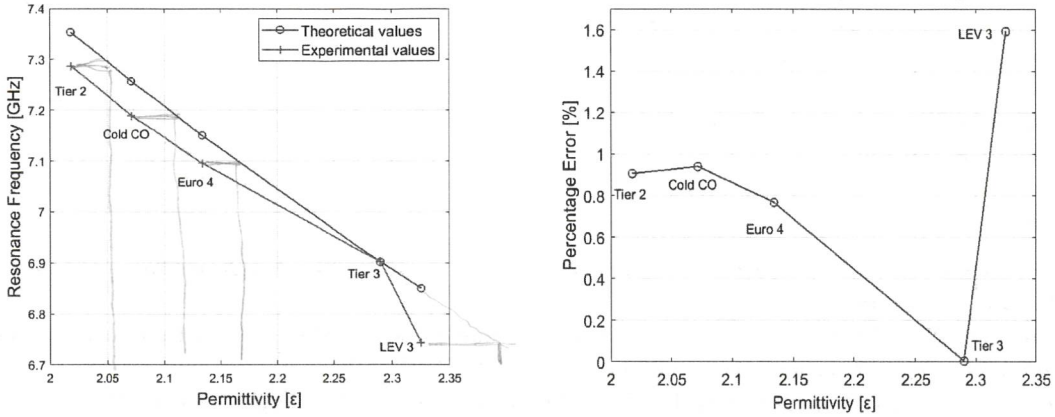

(a) **(b)**

Figure 12. (a) Theoretical and experimental results of the proposed sensor for different gasoline samples at 20°C temperature. **(b)** Percentage error between the theoretical and experimental results of the proposed sensor for different gasoline samples at 20°C temperature.

Sample	DI	Resonant Frequency $f_r[MHz]$	Sensitivity $[100KHz/DI]$	Sample	DI	Resonant Frequency $f_r[mV]$	Sensitivity $[100mV/DI]$
Cold CO	1132	7191.0	51.05	A	1131	2180	0.020
Tier3	1075	6900.0		B	1087	2090	
LEV3	1168	6788.9	11.93	C	1164	2230	0.018
		(a)				**(b)**	

Table 7. Sensitivity/DI **(a)** The proposed RF method **(b)** Capacitor method

5. Conclusion

A cylindrical cavity sensor is proposed to distinguish different DI gasoline for different temperature conditions. The sensing principle relies on the change of resonant frequency caused by the change of permittivity of fuel samples inside cavity sensor. The proposed sensor utilizes circular cavity design which is economical, compact, easy to fabricate, easy to calibrate and sensitive in terms of resonant frequency separation. The performance of the proposed sensor design was verified by HFSS simulations and experiments. The resonant mode chosen for the waveguide is TM_{012} for easier manufacturing as compared to TE. The presented sensor is fabricated with enclosed conductive copper cylinder and a fixed coupling probe wrapped with Teflon mounted inside the top center of the cavity resonator. The experimental results are in agreement with theoretical results which showed the accuracy of the proposed sensor. The novel contribution of presented sensor is its robust behavior under temperature variations and still achieving reasonable resonant frequency separation for different gasoline samples with very small difference in permittivities. Therefore, it can be concluded that the presented sensor can be effectively used to distinguish gasoline with different DI and has potential applications.

Acknowledgments: This research was supported by Basic Science Research Program through the National Research Foundation of Korea (NRF) funded by the Ministry of Science, ICT Future Planning (No.NRF-2017R1A2B4003705)

Conflicts of Interest: The authors declare no conflict of interests

Abbreviations

The following abbreviations are used in this manuscript:

HiDI	High Driveability Index
HFSS	High Frequency Structure Simulator
VNA	Vector Network Analyzer
TE	Transverse Electric
TM	Transverse Magnetic

References

1. David C. Tamm, Gary N. Devenish, Daniel R. Finelt, Amelia L. Kalt. Analysis of Gasoline Octane Costs. [*U.S. Energy Information Administration*]. **2018**, 10–11.
2. Jewitt, Carlton H., Lewis M. Gibbs, and Beth Evans. Gasoline driveability index, ethanol content and cold-start/warm-up vehicle performance. *SAE transactions*, **2005**: 1707-1719.
3. B. Evans, S. Jorgensen, G. Nusser, K. Eng, M. McNally, C. Richardson, D. Whelan, E. Ziegel, New fuel volatility indices, *Automot. Eng.*, pp. 175-176, Feb. **2000**.
4. Lee, Han-Sheng, Simon S. Wang, David K. Lambert, Jack Yingjie Lin, and Charles R. Harrington. An on-vehicle fuel driveability index sensor. *IEEE Sensors Journal 4, no. 6*, **2004**: 722-727.
5. Lambert, D., Harrington, C., Kerr, R., Lee, H. et al., Fuel Driveability Index Sensor, *SAE Technical Paper* 2003-01-3238, **2003**
6. Ferguson, Todd J., Joseph R. Griffin, and Francis De Blauwe. High DI fuel detection via exhaust gas temperature measurement for ULEV. No. 2000-01-0893. *SAE Technical Paper*, **2000**.
7. Naik, Himanshu, Daryl J. Murry, L. E. Kirsch, and Lawrence Fleckenstein. Development and validation of a high-performance liquid chromatography–mass spectroscopy assay for determination of artesunate and dihydroartemisinin in human plasma. *Journal of Chromatography B 816*, no. 1-2 **2005**: 233-242.
8. Johnson, Kevin J., Susan L. Rose-Pehrsson, and Robert E. Morris. Monitoring diesel fuel degradation by gas chromatography mass spectroscopy and chemometric analysis. *Energy fuels 18* , no. 3 **2004**: 844-850.
9. A. Babajanyan, J. Kim, S. Kim, K. Lee, B. Friedman, Sodium chloride sensing by using a near-field microwave microprobe, *Appl. Phys. Lett., vol. 89*, no. 18, pp. 183504-1-183504-3, **2006**.
10. Gennarelli, Gianluca, Stefania Romeo, Maria Rosaria Scarfi, and Francesco Soldovieri. A microwave resonant sensor for concentration measurements of liquid solutions. *IEEE Sensors Journal 13*, no. 5 **2013**: 1857-1864.
11. M. Hofmann, G. Fischer, R. Weigel, D. Kissinger. Microwave-Based noninvasive concentration measurements for biomedical applications. *IEEETrans. Microw. Theory Tech., 61*, **2013** pp. 2195–2204.
12. Arshad.Hassan, KiBae Lee, Jinho Bae, Chong Hyun Lee. An inkjet-printed micro strip patch sensor for liquid identification. *Sens. Actuators A: Phys*, **2017**
13. Kiani, Sina, Pejman Rezaei, Moein Navaei, and Mohammad Sadegh Abrishamian. Microwave sensor for detection of solid material permittivity in single/multilayer samples with high quality factor. *IEEE Sensors Journal 18*, no. 24 **2018**: 9971-9977.
14. Guo, Hongfu, Lu Yao, and Fen Huang. A cylindrical cavity sensor for liquid water content measurement. *Sensors and Actuators A: Physical* 238 **2016**: 133-139.
15. K. Saeed, R. Pollard, I. C. Hunter, Substrate integrated waveguide cavity resonator for complex permittivity characterization of materials, Trans. Microw. Theory Tech., vol. 56, no. 10, pp. 2340-2347, Oct. **2008**
16. Cuenca, Jerome A., Daniel R. Slocombe, and Adrian Porch. Temperature correction for cylindrical cavity perturbation measurements. *IEEE Transactions on Microwave Theory and Techniques* 65, no. 6 **2017**: 2153-2161.
17. Xiang Li, Yan Jiang. Design of a Cylindrical Cavity Resonator for Measurements of Electrical Properties of Dielectric Materials. *Master Thesis in Electronics/Telecommunications*, **2010**
18. Zhao zong Meng, Zhipeng Wu and John Gray. Microwave sensor technologies for food evaluation and analysis: Methods, challenges and solutions. *Transactions of the Institute of Measurement and Control 40* no. 12 **2018**: 3433-3448
19. Meitzler, Allen H., and George S. Saloka. Two alternative, dielectric-effect, flexible-fuel sensors. *SAE transactions*, **1992**: 1455-1466.
20. Oon, Cheen Sean, Muhammad Ateeq, Andy Shaw, Stephen Wylie, Ahmed Al-Shamma'a, and Salim Newaz Kazi. Detection of the gas–liquid two-phase flow regimes using non-intrusive microwave cylindrical cavity sensor. *Journal of Electromagnetic Waves and applications* 30, no. 17 **2016**: 2241-2255.

21. Oon, C. S., M. Ateeq, A. Shaw, A. Al-Shamma'a, S. N. Kazi, and A. Badarudin. Experimental study on a feasibility of using electromagnetic wave cylindrical cavity sensor to monitor the percentage of water fraction in a two phase system. *Sensors and Actuators A: Physical* 245 **2016**: 140-149.
22. Zinal, Sherko, and Georg Boeck. Complex permittivity measurements using TE/sub 11p/modes in circular cylindrical cavities. *IEEE transactions on microwave theory and techniques* 53, no. 6 **2005**: 1870-1874.
23. Jensen, Erk. Rf cavity design. *arXiv preprint arXiv:1601*.05230 **2016**.
24. Jim Frusti, Chrysler, California LEVIII Certification Fuel Gasoline. ARB Public Workshop, El Monte, Calif - Alliance Fuels Group Comments, delivered July 19, **2011**
25. Wikipedia contributors. (2019, August 15). European emission standards. In *Wikipedia, The Free Encyclopedia*. Retrieved 09:05, August 28, **2019**, link
26. Dielectric Constants of Common Materials, In *KAB Electro Acoustics*, link
27. Carey AA, Hayzen AJ. Machinery lubrication - The Dielectric Constant and Oil Analysis. Emerson Process Management, August **2013**, link
28. Bezman, Richard D., Edward F. Casassa, and Robert L. Kay. The temperature dependence of the dielectric constants of alkanols. *Journal of molecular liquids* 73 **1997**: 397-402.
29. Standard for Fuel Systems in Fuel Cell and Other Hydrogen Vehicles. *SAE International J2579*, **2013**
30. A. Mason, B. Abdullah, M. Muradov, O. Korostynska, A. Al-Shamma'a, S.G. Bjarnadottir, K. Lunde, O. Alvseike. Theoretical basis and application for measuring pork loin drip loss using microwave spectroscopy, *Sensors* 16 **2016**: 1–13.

© 2019 by the author. Submitted to *Sensors* for possible open access publication under the terms and conditions of the Creative Commons Attribution (CC BY) license (http://creativecommons.org/licenses/by/4.0/).